Bioorganic & Medicinal Chemistry Letters 20 (2010) 1752–1757

Contents lists available at ScienceDirect

Bioorganic & Medicinal Chemistry Letters

journal homepage: www.elsevier.com/locate/bmcl

Synthesis, SAR and intramolecular hydrogen bonding pattern of 1,3,5-trisubstituted 4,5-dihydropyrazoles as potent cannabinoid CB_1 receptor antagonists

Jos H. M. Lange *, Martina A. W. van der Neut, Arnold P. den Hartog, Henri C. Wals, Jan Hoogendoorn, Herman H. van Stuivenberg, Bernard J. van Vliet, Chris G. Kruse

Solvay Pharmaceuticals, Research Laboratories, Chemical Design & Synthesis Unit, C. J. van Houtenlaan 36, 1381 CP Weesp, The Netherlands

ARTICLE INFO

Article history:
Received 17 November 2009
Revised 5 January 2010
Accepted 6 January 2010
Available online 20 January 2010

Keywords:
Cannabinoid
CB1 receptor
Antagonist
Inverse agonist
Pharmacophore
Intramolecular hydrogen bonding
Scaffold hopping
X-ray diffraction
Absolute configuration
Fluorination
Crystallography

ABSTRACT

The synthesis, structure–activity relationship (SAR) studies and intramolecular hydrogen bonding pattern of 1,3,5-trisubstituted 4,5-dihydropyrazoles are described. The target compounds **6**–**18** represent a novel class of potent and selective CB_1 receptor antagonists. Based on X-ray diffraction data, the orally active **17** is shown to elicit a different intramolecular H-bonding mode as compared to ibipinabant (**3**) and SLV330 (**4**).

The endocannabinoid system plays an important role in many physiological processes.[1] In particular, cannabinoid CB_1 receptor antagonists/inverse agonists have shown clinical efficacy in the treatment of obesity and related cardiovascular and metabolic risk factors,[2,3] and have also been related[4,5] to the potential treatment of addiction, cognitive disorders and peripherally mediated disorders like liver fibrosis, cancer, arthritis and chronic bronchitis. Although the risk of psychiatric side-effects has terminated[6] many development programs of CB_1 receptor blockers for obesity, suggestions have been made to focus on possible therapeutic applications in peripheral pathologies[7] and even for continuing obesity clinical trials while safeguarding the safety of patients and clinical trial subjects.[8] The majority of the reported[9] CB_1 receptor antagonists and inverse agonists can be described in terms of a general pharmacophore model.[10–14]

In considering options for designing novel classes of orally active and CB_1/CB_2 subtype selective cannabinoid CB_1 receptor antagonists, the pyrazolines **1**–**4** were chosen as a starting point. It was anticipated that a regioisomeric shift of the pyrazoline ring in the compounds **1**–**4** would lead to a novel chemotype of CB_1 receptor antagonists. As a matter of fact Solvay was the first[15] to patent this principle. More recently, researchers from Esteve specifically claimed[16] the optically active **5**—which contains the same *N*-piperidinylcarboxamide moiety and aryl-chloro-substitution pattern as rimonabant—in a patent application and demonstrated its in vivo activity in an obesity model. Its 5*S* configuration is remarkable since—based on the absolute configurations of ibipinabant[17] **3** and **4**[18] and their resulting threedimensional (^{3}D) geometries—the 5*R* configuration would at forehand be expected for **5**. Srivastava et al. also embarked[19] on carboxamides and hydrazides related to **5** but did not disclose the absolute configurations of their compounds. These findings prompted us to synthesize and disclose our results of target compounds[20] **6**–**18**. The activities of these novel 1,3,5-trisubstituted 4,5-dihydropyrazoles were compared with their 1,3,4-trisubstituted counterparts **1**–**4** and a set of novel analogues **19**–**25**. The focus in this study was directed to the stereochemical aspects of the resulting CB_1 receptor-ligand interactions as well as on the potential role of intramolecular H-bonding interactions in these structures. In addition, the impact of

* Corresponding author. Tel.: +31 (0)294 479731; fax +31 (0)294 477138.
E-mail address: jos.lange@solvay.com (J.H.M. Lange).

0960-894X/$ - see front matter © 2010 Elsevier Ltd. All rights reserved.
doi:10.1016/j.bmcl.2010.01.049

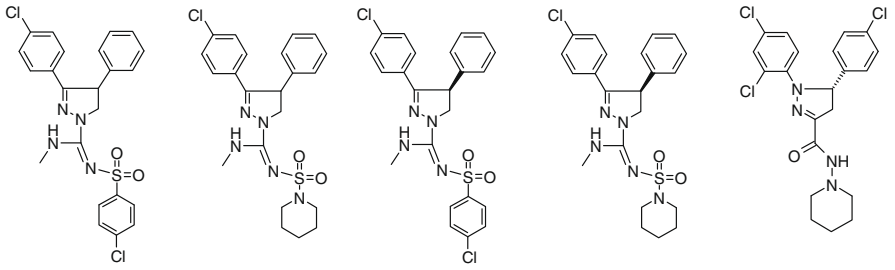

1 **2** **3** **4** **5**

fluorination[21–23] at the piperidine moiety of **2** was studied since this recently[24] led to retained CB_1 antagonism in the structurally related 1,4,5,6-tetrahydropyridazine series.

The target compounds **6–18** have been synthesized as depicted in Scheme 1. Diazotation of the anilines **26** and **27**, followed by reaction[25] with ethyl 2-chloro-3-oxobutanoate gave **28** and **29**, respectively. Subsequent ring closure with styrene under basic conditions at elevated temperature afforded the 3-pyrazoline esters **29** and **30** in high yields. These esters **29** and **30** were hydrolyzed under basic conditions into the carboxylic acids **31** and **32**, which were subsequently chlorinated with $SOCl_2$. The in situ formed acid chlorides were reacted efficiently with aromatic sulfonamides under basic conditions to give the intermediates **33–37**. The target compounds **6–10** were obtained in varying yields by a chlorination reaction with PCl_5 at elevated temperature from **33–37**, followed by treatment with $CH_3NH_2{\cdot}HCl$ in the presence of Hünig's base. The key precursor **31** was converted analogously to crude **38–41** in quantitative yields. The conversion of the obtained crude **39–41** into the target compounds **12–14** was performed under milder chlorination conditions ($POCl_3$/DMAP, 40 °C) which

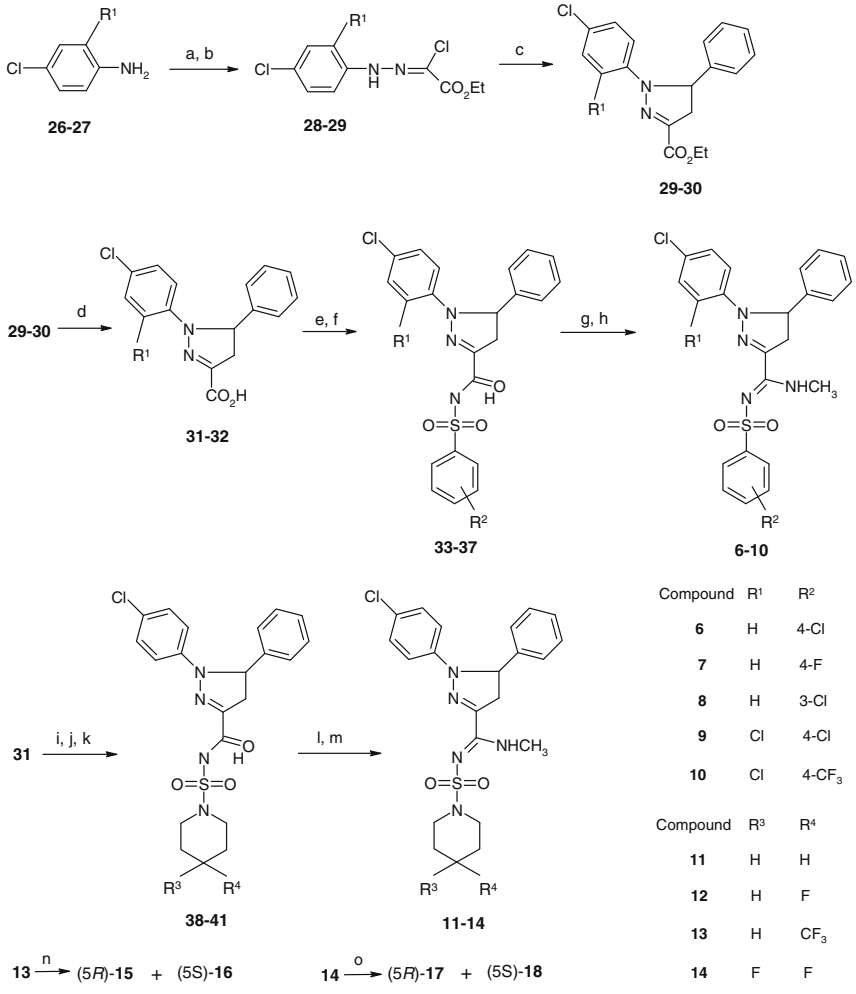

Compound	R^1	R^2
6	H	4-Cl
7	H	4-F
8	H	3-Cl
9	Cl	4-Cl
10	Cl	4-CF_3

Compound	R^3	R^4
11	H	H
12	H	F
13	H	CF_3
14	F	F

Scheme 1. Reagents and conditions: (a) $NaNO_2$, HCl, H_2O, 0–5 °C, 1 h; (b) ethyl 2-chloro-3-oxobutanoate, NaOAc, EtOH, rt, 16 h (65–73%); (c) styrene, Et_3N, benzene, reflux, 1 h (94–97%); (d) NaOH, MeOH, H_2O, reflux, 2 h (78–91%); (e) $SOCl_2$, toluene, 80 °C, 1 h; (f) $R_2C_6H_4SO_2NH_2$, CH_3CN, NaOH, rt, 16 h (78–90%); (g) PCl_5, chlorobenzene, 140 °C, 90 min; (h) $CH_3NH_2{\cdot}HCl$, DIPEA, CH_2Cl_2, rt, 1 h (15–23%); (i) $SOCl_2$, toluene, 80 °C, 1 h; (j) 4,4-R^3R^4-piperidine-1-sulfamide, NaH, CH_3CN, rt, 16 h; (k) 1 N HCl, CH_2Cl_2, rt, 1 h; (l) for **11**: PCl_5, chlorobenzene, 140 °C, 90 min; for **12–14**: $POCl_3$, DMAP, CH_2Cl_2, reflux, 4 h; (m) $CH_3NH_2{\cdot}HCl$, DIPEA, CH_2Cl_2, 6 °C to rt, 16 h (49–88%); (n) 250 × 30 mm CHIRALPAK® AD-H 5 μm column, mobile phase: 70/30 CO_2/ethanol + 1% Et_2NH (supercritical fluid chromatography), flow rate: 120 ml/min; 25 °C, detection: UV 250 nm, outlet pressure: 130 bars; (o) 250 × 76 mm CHIRALPAK® T-101 column, mobile phase: $CH_3OH/CH_3CN/Et_2NH$ = 84.9/15/0.1 (v/v), flow rate: 250 ml/min; 25 °C, detection: UV 220 nm.

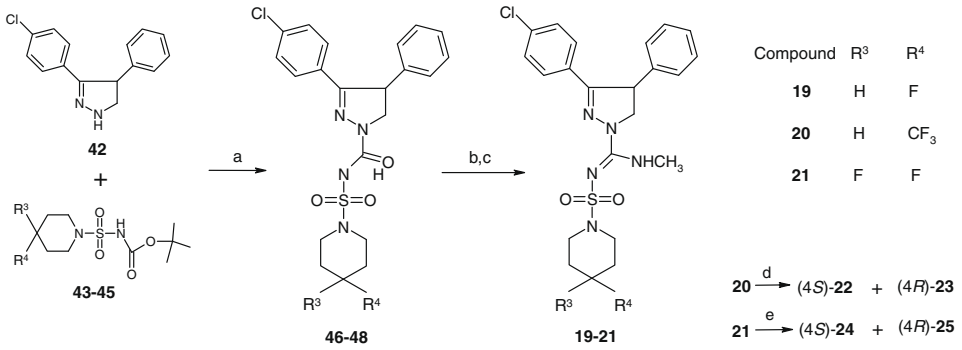

Scheme 2. Reagents and conditions: (a) toluene, reflux, 3 h; (b) $POCl_3$, DMAP, CH_2Cl_2, reflux, 4 h (70–80%); (c) CH_3NH_2·HCl, DIPEA, 6 °C to rt, 16 h (85–91%); (d) 250 × 76 mm CHIRALPAK® AD 20 μm column, mobile phase: CH_3OH/CH_3CN = 50/50 (v/v), flow rate: 270 ml/min; 25 °C, detection: UV 250 nm; (e) 250 × 80 mm CHIRALPAK® AD 20 μm column, mobile phase: CH_3OH/CH_3CN = 90/10 (v/v), flow rate: 200 ml/min; 25 °C, detection: UV 230 nm.

resulted in significantly higher yields as compared to the conversion of **38** into **11**, which was synthesized by applying the conventional reaction conditions (PCl_5, elevated temperature). To further investigate the stereochemical requirements for binding to the CB_1 receptor in this chiral pyrazoline series in more detail, the key compounds **13** and **14** were separated into their enantiomers by using chiral preparative HPLC to furnish two sets of compounds **15**/**16** and **17**/**18**, respectively.

Coupling of the dihydropyrazole building block[26] **42** with the carbamate esters[24] **43**–**45** afforded **46**–**48** in 70–80% yield, which was successively chlorinated with $POCl_3$ in the presence of DMAP and reacted with CH_3NH_2·HCl in the presence of Hünig's base to furnish the target compounds **19**–**21** in high yields (Scheme 2). The chiral compounds in this series **20** and **21** were separated into their enantiomers by using chiral preparative HPLC to furnish two sets of compounds **22**/**23** and **24**/**25**, respectively.

The pharmacological results of the compounds **1**–**4** and **6**–**25** are given in Table 1. They were evaluated in vitro at the human CB_1 and CB_2 receptor, stably expressed into Chinese Hamster Ovary (CHO) cells,[17] utilizing radioligand binding studies (displacement of the specific binding of [^{3}H]-CP-55,940). CB_1 receptor antagonism[17] was measured using a CP-55,940 induced arachidonic acid release functional assay, using the same recombinant cell line. In vivo activities of a set of key compounds after oral administration was investigated in a CB agonist-induced rat hypotension model.[17]

Comparison of the CB_1 receptor binding data of the novel target compound **6** and its known counterpart **1** revealed that the regioisomeric shift of the pyrazoline ring appeared to have some negative effect on the CB_1 receptor affinity of **6** (Table 1), although it should be noted that the CB_1 affinity SEM value of **6** is relatively high. However, in the case of their piperidinyl derivatives **11** and **2**, respectively, no significant impact on CB_1 receptor affinity was observed. Comparison of the CB_1 receptor affinities of the target compounds **6** and **9** showed a positive effect of the additional 2-Cl atom in **9**. In this arylsulfonyl series **6**–**10**, the CF_3-substituted **10** showed the highest CB_1 receptor affinity (11.3 nM). However,

Table 1
Pharmacological in vitro and in vivo results of compounds **1**–**4** and **6**–**25**

Compound	K_i (CB_1)[a], nM	pA_2 (CB_1)[b]	K_i (CB_2)[c], nM	CB_1/CB_2 ratio	Hypotension rat[d], ID_{50}
1	25.2 ± 7.4	8.7 ± 0.3	>1000	>39	15
2	152 ± 68	8.7 ± 0.3	1321 ± 264	8.6	n.d.[e]
3	7.8 ± 1.4	9.9 ± 0.6	7943 ± 126	1018	5.5
4	58 ± 19	8.7 ± 0.2	3495 ± 968	60	8
6	84 ± 56	8.4 ± 0.3	>1000	>11	>30
7	21.7 ± 10.0	8.0 ± 0.3	>1000	>46	30
8	53 ± 10	8.3 ± 0.2	330 ± 171	6	>30
9	37 ± 23	9.0 ± 0.1	248 ± 96	7	>30
10	11.3 ± 2.0	8.6 ± 0.1	179 ± 38	16	>30
11	141 ± 58	7.9 ± 0.2	1086 ± 86	8	>30
12	55 ± 16	8.4 ± 0.2	>1000	>18	>30
13	7.6 ± 2.0	9.4 ± 0.3	606 ± 204	84	n.d.[e]
14	38.8 ± 14.0	9.1 ± 0.6	>1000	>25	9
15	2.0 ± 1.0	9.5 ± 0.1	584 ± 220	292	n.d.[e]
16	58 ± 22	8.2 ± 0.1	>1000	>17	n.d.[e]
17	9.2 ± 2.0	8.8 ± 0.1	>1000	>108	5
18	280 ± 81	<6.7	>1000	>3.5	>30
19	7.5 ± 4.3	9.0 ± 0.2	>1000	>133	>30
20	14.5 ± 11.9	9.4 ± 0.1	>1000	>68	n.d.[e]
21	12.2 ± 5.0	9.2 ± 0.3	219 ± 91	18	23
22	4.7 ± 1.7	9.6 ± 0.1	305 ± 58	65	2
23	140 ± 60	7.3 ± 0.2	>1000	>7	>30
24	42 ± 24	9.0 ± 0.1	>1000	>23	6
25	463 ± 168	6.4 ± 0.2	>1000	>2	>30

[a] Displacement of specific CP-55,940 binding in CHO cells stably transfected with human CB_1 receptor, expressed as K_i ± SEM (nM).
[b] [^{3}H]-Arachidonic acid release in CHO cells expressed as pA_2 ± SEM values.
[c] Displacement of specific CP-55,940 binding in CHO cells stably transfected with human CB_2 receptor, expressed as K_i ± SEM (nM). The values represent the mean result based on at least three independent experiments.
[d] Antagonism of CB agonist (CP-55,940) induced hypotension (rat), expressed as ID_{50} (mg/kg, po administration).
[e] n.d. = not determined.

the presence in **10** of the additional 2-Cl substituent in combination with the CF_3 group led also to a highly lipophilic[27] compound ($A \log P$[28] = 5.9). Compound **7** elicited the highest CB_1/CB_2 receptor selectivity in this set of compounds.

Significant differences exist in the SAR between the 1,3,4-trisubstituted pyrazoline class and the 1,3,5-trisubstituted pyrazoline class. For example, in the novel 1,3,5-trisubstituted pyrazoline series, the 4-F substituted **7** showed a fourfold higher CB_1 receptor affinity than its 4-Cl analogue **6**. In contrast, in the earlier reported[17] 1,3,4-trisubstituted pyrazoline series the 4-Cl substituted **1** showed a 13-fold higher CB_1 receptor affinity than its 4-F substituted counterpart (cf. compounds **67** and **72**, respectively, in Ref. 17). Such a marked difference in SAR cannot be rationalized based on the reported[10–14] CB_1 inverse agonist pharmacophore model but is an indicator for distinct structural differences between both classes of pyrazolines. One of the aims of this investigation was the identification of relevant factors involved herein.

In the piperidinylsulfonyl-derived series **11**–**14**, the CF_3-substituted **13** elicited the highest CB_1 receptor affinity and functional CB_1 antagonistic potency. Comparison of the regioisomeric pairs **12**/**19** and **14**/**21** showed that the CB_1 receptor affinities are higher in the 1,3,4-trisubstituted pyrazoline series. However, the opposite was observed for **13** and **20**, respectively. In particular, the compounds **13** and **19** share high CB_1 receptor affinity values with high CB_1/CB_2 subtype selectivities and strong CB_1 antagonistic potencies.

Since **13** and **14** are racemates their enantiomerically pure constituents were also tested. In both cases the dextrorotatory enantiomers **15** and **17** had significantly higher CB_1 receptor affinities and CB_1 antagonistic potencies than their levorotatory counterparts **16** and **18**. The highest CB_1 receptor affinity (2.6 nM) was found in the eutomer **15**. The distomer **16** showed ~30-fold less CB_1 affinity than the eutomer **15**, indicating that these chiral ligands bind stereoselectively to the CB_1 receptor. A comparable degree of stereoselective binding to the CB_1 receptor was observed for the 1,3,4-pyrazoline counterparts **22** and **23**. The distomer **18** showed ~30-fold less CB_1 affinity than **17**, but in this case the corresponding 1,3,4-pyrazoline counterparts **25** and **24** elicited not more than an 11-fold difference in CB_1 receptor affinity.

Interestingly, the impact of variation in stereochemistry on the observed CB_1 receptor affinities in our sulfonylamidine-based series of 1,3,5-trisubstituted 4,5-dihydropyrazoles appears to be considerably higher (~30-fold ratio for the compound sets **15**/**16** and **17**/**18**, respectively) as compared with the hydrazide-based compounds,[19] such as the reported analogue of **5** wherein its piperidinyl moiety was substituted by a 4-morpholinyl group (~threefold difference).

The in vivo activity after oral administration was investigated in a CB_1 agonist (CP-55,940) induced hypotension rat model.[17] Disappointingly, our initially prepared set of arylsulfonyl-based target compounds **6**–**10** were hardly active or inactive in this model, whereas compound **1** previously had shown significant activity therein. Therefore, we focused our attention on the piperidine-based compound **11**, but this compound was also found inactive after oral administration. Based on molecular modeling studies it became apparent that the CB_1 receptor would accommodate an additional substituent at the 4-position of the piperidine ring of **11**. This prompted the design of the compounds **12**–**14**. Gratifyingly, the 4,4-difluoro substituted **14** in this series was found orally active (ID_{50} = 9 mg/kg). According to expectation, its related eutomer **17** was approximately twofold more active in this model after oral administration (ID_{50} = 5 mg/kg). In our piperidinylsulfonyl-based 1,3,4-trisubstituted pyrazoline series we also identified some novel compounds with a high oral activity. The 4,4-difluoro substituted **24** (ID_{50} = 6 mg/kg) and in particular the 4-CF_3 substituted **22** (ID_{50} = 1.9 mg/kg) were found very active in our mechanistic in vivo rodent model after oral administration. It is interesting to note that **22** was found more potent in this model than ibipinabant (**3**), as well as rimonabant[17] (ID_{50} = 3.2 mg/kg).

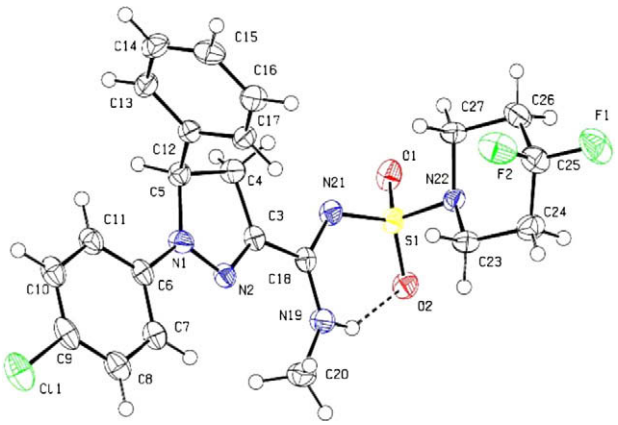

Figure 1. ORTEP drawing of the X-ray diffraction result of **17**. Its intramolecular H-bond is indicated as a dashed line.

The effects of intramolecular H-bonding on pharmacodynamic and pharmacokinetic properties of drugs are a known phenomenon.[29–31] Intramolecular H-bonding in general decreases the polar surface area, thereby enhancing the membrane permeability and consequently improving oral absorption. It also generally results in a somewhat higher degree of conformational constraint as compared to structural analogues lacking such an intramolecular binding feature. The comparison of the X-ray diffraction structure of **17** with the earlier reported X-ray diffraction results of compounds **3**[17] and **4**[18], respectively, showed that intramolecular H-bonding is present in both structure types. Both the Flack x parameter[32] value (-0.06 ± 0.04) and the independent analysis of the data in terms of the Hooft parameter[33] (-0.028 ± 0.016) indicated an enantiomerically pure crystal of **17** with a high level of confidence. Unexpectedly, a clear difference in intramolecular H-bonding exists between the two sets of pyrazoline chemotypes. Apparently, the different sprouting of the three substituents from the common pyrazoline scaffold in **3** and **4** on the one hand and **17** on the other hand has a large impact on their preferred intramolecular H-bonding modes. An intramolecular H-bond interaction between the pyrazoline N_2 atom and its amidine N–H hydrogen atom was present in both **3** and **4**, whereas a strong intramolecular H-bond interaction between one of the oxygen atoms of the sulfonyl group and its amidine N–H hydrogen atom was observed in **17** (Fig. 1). The difference in intramolecular H-bond formation between the two sets of compounds can be rationalized by invoking the different inter-atom distance between the pyrazoline C_3 atom and the amidine C atom in **17** (1.46 Å) as compared to the pyrazoline N_1 atom and the amidine C atom in **3** (1.36 Å), respectively. The shorter distance in **3** can be explained by a higher degree of conjugation between its carboxamidine moiety and the pyrazoline ring, thereby resulting in partial double bond character and a shorter bond length. These shorter bond lengths in **3** and **4**, as well as differences in their overall molecular geometry—due to their differently substituted pyrazoline ring—as compared to **17**, apparently facilitate the specific intramolecular H-bond as shown in Figure 2. The observed differences in SAR described hereinabove between some corresponding members of the two pyrazoline classes can be rationalized by invoking differences in the resulting ^{3}D shapes, as a result of different modes of intramolecular H-bonding. More specific, an analogous orientation of both pyrazoline-bound aromatic moieties and one of the sulfonyl-oxygen atoms (which is supposed[10] to form a key interaction with the Lys192 residue of the CB_1 receptor via H-bonding) at the CB_1 receptor will lead to a different positioning

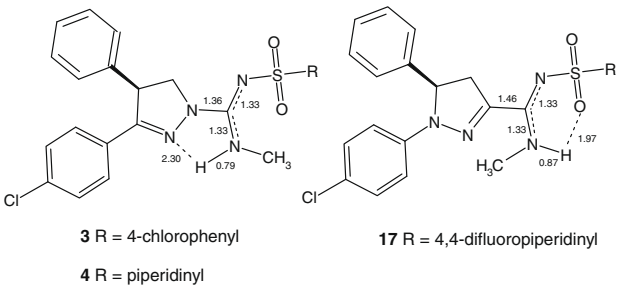

Figure 2. Schematic representation of the intramolecular H-bonding pattern in the compounds **3** and **4** versus **17**. The depicted inter-atom distances for **3** and **17** from their X-ray diffraction analyses are expressed in Å.

of both their amidine N–CH_3 substituent and the hydrophobic piperidine region therein. It should be noted that the presence of an alternative hydrophobic pocket in the CB_1 receptor has been suggested earlier.[34]

Surprisingly, the key compound **17** showed the opposite absolute configuration as compared to Esteve's **5**. Both compounds would be expected to bind analogously to the CB_1 receptor, based on the published[10–14] CB_1 inverse agonist pharmacophore model, since their pyrazoline moieties are almost identical and an H-acceptor moiety is present in their lipophilic tail region. It should be borne in mind that both the size and nature of their tails (N-piperidinylcarboxamide in **5** vs 4,4-difluoropiperidinyl-sulfonylcarboxamidine in **17**) is different which can lead to different preferential binding modes[14] at the CB_1 receptor. Additional sophisticated molecular modeling investigations will be mandatory to provide a clear explanation for these observations.

Novel 1,3,5-trisubstituted 4,5-dihydropyrazoles are described. The target compounds[35] **6**–**18** represent a novel class of potent and selective CB_1 receptor antagonists. Although the key compound **17** showed the opposite absolute configuration—according to the Cahn-Ingold-Prelog rules—as compared to **3** and **4**, the stereochemical orientation of the relevant side chains for CB_1 receptor binding in **17** matched the orientation of the corresponding substituents in **3** and **4**. The orally active **17** was shown to elicit a different intramolecular H-bonding pattern as compared to **3** and **4**. The observed clear differences in SAR described hereinabove between some corresponding members of the two pyrazoline classes was rationalized by invoking differences in ^{3}D shape, as a result of different modes of intramolecular H-bonding as well as the different attachment points of the three substituent at their pyrazoline ring.

Acknowledgments

Jan Jeronimus and Hugo Morren are gratefully acknowledged for supply of the analytical data.

References and notes

1. Lambert, D. M.; Fowler, C. J. *J. Med. Chem.* **2005**, *48*, 5059.
2. van Gaal, L. F.; Rissanen, A. M.; Scheen, A. J.; Ziegler, O.; Roessner, S. *Lancet* **2005**, *365*, 1389.
3. Antel, J.; Gregory, P. C.; Nordheim, U. *J. Med. Chem.* **2006**, *49*, 4008.
4. Lange, J. H. M.; Kruse, C. G. *Chem. Rec.* **2008**, *8*, 156.
5. Di Marzo, V. *Nat. Rev. Drug Disc.* **2008**, *7*, 438.
6. Jones, D. *Nat. Rev. Drug Disc.* **2008**, *7*, 961.
7. Bifulco, M.; Pisanti, S. *Nat. Rev. Drug Disc.* **2009**, *8*, 594.
8. Le Foll, B.; Gorelick, D. A.; Goldberg, S. R. *Psychopharmacology* **2009**, *205*, 171.
9. Högenauer, E. K. *Exp. Opin. Ther. Patents* **2007**, *17*, 1457.
10. Reggio, P. H. *Curr. Pharm. Des.* **2003**, *9*, 1607.
11. Lange, J. H. M.; Kruse, C. G. *Curr. Opin. Drug Discovery Dev.* **2004**, *7*, 498.
12. Lange, J. H. M.; Kruse, C. G. *Drug Discovery Today* **2005**, *10*, 693.
13. Wang, H.; Duffy, R. A.; Boykow, G. C.; Chackalamannil, S.; Madison, V. S. *J. Med. Chem.* **2008**, *51*, 2439.
14. Foloppe, N.; Benwell, K.; Brooks, T. D.; Kennett, G.; Knight, A. R.; Misra, A.; Monck, N. J. T. *Bioorg. Med. Chem. Lett.* **2009**, *19*, 4183.
15. Lange, J. H. M.; Kruse, C. G.; Van Stuivenberg, H. H. WO2005/074920, 2005.
16. Cuberes Altisen, R. EP1743892, 2007.
17. Lange, J. H. M.; Coolen, H. K. A. C.; van Stuivenberg, H. H.; Dijksman, J. A. R.; Herremans, A. H. J.; Ronken, E.; Keizer, H. G.; Tipker, K.; McCreary, A. C.; Veerman, W.; Wals, H. C.; Stork, B.; Verveer, P. C.; den Hartog, A. P.; de Jong, N. M. J.; Adolfs, T. J. P.; Hoogendoorn, J.; Kruse, C. G. *J. Med. Chem.* **2004**, *47*, 627.
18. Lange, J. H. M.; van Stuivenberg, H. H.; Veerman, W.; Wals, H. C.; Stork, B.; Coolen, H. K. A. C.; McCreary, A. C.; Adolfs, T. J. P.; Kruse, C. G. *Bioorg. Med. Chem. Lett.* **2005**, *15*, 4794.
19. Srivastava, B. K.; Joharapurkar, A.; Raval, S.; Patel, J. Z.; Soni, R.; Raval, P.; Gite, A.; Goswami, A.; Sadhwani, N.; Gandhi, N.; Patel, H.; Mishra, B.; Solanki, M.; Pandey, B.; Jain, M. R.; Patel, P. R. *J. Med. Chem.* **2007**, *50*, 5951.
20. Lange, J. H. M.; den Hartog, A. P.; van Vliet, B. J. WO2009/130234, 2009.
21. Purser, S.; Moore, P. R.; Swallow, S.; Gouverneur, V. *Chem. Soc. Rev.* **2008**, *37*, 320.
22. Hagmann, W. K. *J. Med. Chem.* **2008**, *51*, 4359.
23. Filler, R.; Saha, R. *Future Med. Chem.* **2009**, *1*, 777.
24. Lange, J. H. M.; den Hartog, A. P.; van der Neut, M. A. W.; Kruse, C. G. *Bioorg. Med. Chem. Lett.* **2009**, *19*, 5675.
25. Shawali, A. S.; Elsheikh, S.; Parkanyi, C. *J. Heterocycl. Chem.* **2003**, *40*, 207.
26. Grosscurt, A. C.; Van Hes, R.; Wellinga, K. *J. Agric. Food. Chem.* **1979**, *27*, 406.
27. Leeson, P. D.; Springthorpe, B. *Nat. Rev. Drug Disc.* **2007**, *6*, 881.
28. Ghose, A. K.; Viswanadhan, V. N.; Wendoloski, J. J. *J. Phys. Chem. A* **1998**, *102*, 3762.
29. Sasaki, S.; Cho, N.; Nara, Y.; Harada, M.; Endo, S.; Suzuki, N.; Furuya, S.; Fujino, M. *J. Med. Chem.* **2003**, *46*, 113.
30. Mire, D. E.; Silfani, T. N.; Pugsley, M. K. *J. Cardiovasc. Pharmacol.* **2005**, *46*, 585.
31. Kasagami, T.; Kim, I.-H.; Tsai, H.-J.; Nishi, K.; Hammock, B. D.; Morisseau, C. *Bioorg. Med. Chem. Lett.* **2009**, *19*, 1784.
32. Flack, H. D. *Acta Crystallogr., Sect. A* **1983**, *39*, 876.
33. Hooft, R. W. W.; Straver, L. H.; Spek, A. L. *J. Appl. Crystallogr.* **2008**, *41*, 96.
34. Carpino, P. A.; Griffith, D. A.; Sakya, S.; Dow, R. L.; Black, S. C.; Hadcock, J. R.; Iredale, P. A.; Scott, D. O.; Fichtner, M. W.; Rose, C. R.; Day, R.; Dibrino, J.; Butler, M.; DeBartolo, D. B.; Dutcher, D.; Gautreau, D.; Lizano, J. S.; O'Connor, R. E.; Sands, M. A.; Kelly-Sullivan, D.; Ward, K. M. *Bioorg. Med. Chem. Lett.* **2006**, *16*, 731.
35. Yields refer to isolated pure products unless otherwise noted and were not maximized. Selected data for compounds **14**, **15**, **17**, **22** and **24**. *Synthesis of compound* **14**: To a stirred solution of **26** (15.68 g, 0.123 mol) in ice (30 ml) and concentrated HCl (30 ml) was slowly added a solution of $NaNO_2$ (9.0 g, 0.13 mol) in H_2O (16 ml) and the resulting solution was stirred for 1 h at 0–5 °C and subsequently added to a cold mixture of NaOAc (32 gram, 0.39 mol), EtOH (520 ml) and ethyl 2-chloro-3-oxobutanoate (16.6 ml, 0.12 mol). After stirring the resulting mixture for 1 h the formed precipitate was collected by filtration, washed with EtOH and dried in vacuo to give **28** (22.99 g, 73% yield). Mp 147.5–149.5 °C. ^{1}H NMR (200 MHz, $CDCl_3$) δ 1.40 (t, J = 7 Hz, 3H), 4.39 (q, J = 7 Hz, 2H), 7.16 (br d, J = 8 Hz, 2H), 7.30 (br d, J = 8 Hz, 2H), 8.31 (br s, 1H). To a stirred boiling solution of **28** (22.95 g, 0.088 mol) and styrene (30.3 ml, 0.264 mol) in benzene (140 ml) was added Et_3N (34.3 ml, 0.247 mol) and the resulting solution was heated at reflux temperature for 1 h. The resulting solution was cooled to rt and the formed precipitate was removed by filtration and washed with toluene. The filtrate was concentrated in vacuo and purified by flash chromatography (silica gel, CH_2Cl_2) to give **29** (27.2 g, 94% yield) as a syrup, which slowly solidified on standing. ^{1}H NMR (200 MHz, $CDCl_3$) δ 1.38 (t, J = 7 Hz, 3H), 3.06 (dd, J = 18 and 7 Hz, 1H), 3.73 (dd, J = 18 and 13 Hz, 1H), 4.33 (q, J = 7 Hz, 2H), 5.38 (dd, J = 13 and 7 Hz, 1H), 7.02 (br d, J = 8 Hz, 2H), 7.08–7.40 (m, 7H). To a stirred suspension of **29** (23.0 g, 0.07 mol) in CH_3OH (200 ml) was added H_2O (15 ml) and concentrated NaOH (10 ml) and the resulting solution was heated at reflux temperature for 2 h. The CH_3OH was partly removed by evaporation and the residue was dissolved in a mixture of H_2O and EtOAc. Ice, concd HCl (20 ml) and EtOAc were successively added, the EtOAc layer collected, dried over $MgSO_4$, filtered and concentrated in vacuo. The resulting residue was washed with Et_2O (100 ml) and diisopropyl ether, respectively, to give **31** as a solid, mp 177–179 °C. To **31** (18.77 g, 62.4 mmol) in toluene (200 ml) was added $SOCl_2$ (18.0 ml, 246.8 mmol). The reaction mixture was stirred at 80 °C for 1 h. Volatiles were thoroughly removed in vacuo. The residue was dissolved in CH_3CN (250 ml): solution A. To a solution of 4,4-difluoropiperidine-1-sulfonamide (12.5 g, 62.4 mmol) in CH_3CN (500 ml) was added aqueous NaOH (8.25 ml, 157.8 mmol). After 10 min, solution A was slowly added. The reaction mixture was stirred overnight at rt. Volatiles were removed in vacuo to give crude **41** (39.01 g). This crude residue was extracted with CH_2Cl_2/1 N HCl. Layers were separated. The CH_2Cl_2 layer was dried over Na_2SO_4, filtered and evaporated to give **41** (30.41 g, quantitative yield). ^{1}H NMR (400 MHz, DMSO-d_6) δ 1.93–2.10 (m, 4H), 2.75 (dd, J = 18 and 6 Hz, 1H), 3.12–3.21 (m, 4H), 3.36 (br s, probably NH and H_2O), 3.62 (dd, J = 18 and 13 Hz, 1H), 5.42 (dd, J = 13 and 6 Hz, 1H), 6.93 (br d, J = 8, 2H), 7.14–7.36 (m, 7H). *Compound* **41** (30.14 g, 62.4 mmol) was dissolved in CH_2Cl_2 (500 ml). DMAP (33.80 g, 276.7 mmol) was added. $POCl_3$ (7.35 ml, 80.3 mmol) in CH_2Cl_2 (50 ml) was added dropwise. The reaction mixture was heated at reflux temperature for 4 h. After cooling down to 6 °C CH_3NH_2·HCl (19.0 g, 281.4 mmol) was added, followed by dropwise addition of DIPEA (72.0 ml, 420.6 mmol). The reaction mixture was stirred overnight at rt. Water (100 ml)

was added, followed by acidification with 1 N HCl. Layers were separated. The CH_2Cl_2 layer was dried over Na_2SO_4, filtered and concentrated in vacuo. Purification by flash chromatography (silica gel, Et_2O/pa (40/60) = 1/1 (v/v)) afforded **14** (27.1 g; 88% yield.) ^{1}H NMR (400 MHz, DMSO-d_6) δ 2.00–2.15 (m, 4H); 2.85 (br d, J ~5 Hz, 3H), 3.09–3.21 (m, 5H), 3.94 (dd, J = 18 and 13 Hz, 1H), 5.61 (dd, J = 13 and 6 Hz, 1H), 7.04 (br d, J = 8, 2H), 7.20–7.38 (m, 7H), 8.80–8.85 m, 1H); ESI$^+$-MS exact mass calcd for $C_{22}H_{25}ClF_2N_5O_2S$ m/z, 496.1386 ([MH$^+$]), found: 496.1411. *Compound* **15**: ^{1}H NMR (400 MHz, DMSO-d_6) δ 1.43–1.60 (m, 2H), 1.83–1.92 (m, 2H), 2.39–2.48 (m, 1H), 2.57–2.69 (m, 2H), 2.88 (br s, 3H), 3.14 (dd, J = 18 and 7 Hz, 1H), 3.60 (t, J = 9 Hz, 2H), 3.94 (dd, J = 18 and 13 Hz, 1H), 5.60 (dd, J = 13 and 7 Hz, 1H), 7.03 (d, J = 9 Hz, 2H), 7.23 (d, J = 9 Hz, 2H), 7.26–7.39 (m, 5H), 8.86 (br s, 1H); ESI$^+$-MS exact mass calcd for $C_{23}H_{26}ClF_3N_5O_2S$ m/z, 528.1448 ([MH$^+$]), found: 528.1475; $[\alpha]_D^{25}$ = 167 (c 1 g/100 ml, CH_3OH). *Compound* **17**: mp 158 °C (EtOH). ^{1}H NMR (400 MHz, DMSO-d_6) δ 2.00–2.15 (m, 4H), 2.85 (br d, J ~5 Hz, 3H), 3.09–3.21 (m, 5H), 3.94 (dd, J = 18 and 13 Hz, 1H), 5.61 (dd, J = 13 and 6 Hz, 1H), 7.04 (br d, J = 8 Hz, 2H), 7.20–7.38 (m, 7H), 8.80–8.85 m, 1H); ESI$^+$-MS exact mass calcd for $C_{22}H_{25}ClF_2N_5O_2S$ m/z, 496.1386 ([MH$^+$]), found: 496.1403; $[\alpha]_D^{25}$ = 165 (c 1 g/100 ml, CH_3OH). *Selected crystallographic data for* **17**: X-ray data were collected under the supervision of Professor Dr. A. L. Spek (Bijvoet Centre for Biomolecular Research, Utrecht University, The Netherlands) with a Nonius KappaCCD diffractometer on a rotating anode using MoKa radiation, temperature: 150 K, crystal size: 0.21 × 0.30 × 0.66 mm, crystal system: monoclinic, space group: $P21$, unit cell dimensions: a = 6.0743; b = 10.4341; c = 17.6350 Å, Calculated density: 1.475 g cm^{-3}. The CIF has been deposited at the Cambridge Crystallographic Data Centre (CCDC), deposition number: 760300. *Compound* **22**: mp 164.5–165 °C. ^{1}H NMR (400 MHz, $CDCl_3$) δ 1.67–1.80 (m, 2H), 1.88–1.95 (m, 2H), 1.99–2.13 (m, 1H), 2.51–2.63 (m, 2H), 3.25 (d, J = 7 Hz, 3H), 3.77–3.86 (m, 2H), 4.10–4.17 (m, 1H), 4.57 (t, J = 11 Hz, 1H), 4.67 (dd, J = 11 and 5.5 Hz, 1H), 6.81 (br s, 1H), 7.15 (d, J = 8 Hz, 2H), 7.23–7.36 (m, 5H), 7.52 (br d, J = 8 Hz, 2H); ESI$^+$-MS exact mass calcd for $C_{23}H_{26}ClF_3N_5O_2S$ m/z, 528.1448 ([MH$^+$]), found: 528.1472; $[\alpha]_D^{25}$ = −130 (c 1 g/100 ml, CH_3OH). *Compound* **24**: mp 185.5–186 °C. ^{1}H NMR (400 MHz, $CDCl_3$) δ 2.03–2.16 (m, 4H), 3.24 (d, J = 7 Hz, 3 H), 3.26–3.34 (m, 4H), 4.14 (dd, J = 12 and 5.5 Hz, 1H), 4.57 (t, J = 12 Hz, 1H), 4.67 (dd, J = 12 and 5.5 Hz, 1H), 6.79 (br s, 1H), 7.15 (d, J = 8 Hz, 2H), 7.23–7.35 (m, 5H), 7.53 (d, J = 8 Hz, 2H); ESI$^+$-MS exact mass calcd for $C_{22}H_{25}ClF_2N_5O_2S$ m/z, 496.1386 ([MH$^+$]), found: 496.1399; $[\alpha]_D^{25}$ = −148 (c 1 g/100 ml, CH_3OH).